Regular Article

PHYSICAL CHEMISTRY RESEARCH
Published by the
Iranian Chemical Society
www.physchemres.org
info@physchemres.org

Phys. Chem. Res., Vol. 12, No. 1, 95-107, March 2024
DOI: 10.22036/pcr.2023.387911.2306

Spectroscopic, Structural and Molecular Docking Studies on N,N-Dimethyl-2-[6-methyl-2-(4-methylphenyl) Imidazo[1,2-a]pyridin-3-yl] Acetamide

A. Ram Kumar, N. Kanagathara and S. Selvaraj*

Institute of Science and Humanities, Saveetha School of Engineering, Saveetha Institute of Medical and Technical Sciences (SIMATS), Thandalam, Chennai, 602105, Tamil Nadu, India

(Received 1 March 2023, Accepted 11 April 2023)

With the help of quantum computational methods, the current study aims to analyze the geometric as well as spectroscopic studies on N,N-dimethyl-2-[6-methyl-2-(4-methylphenyl) imidazo[1,2-a]pyridin-3-yl] acetamide (zolpidem). The optimized structural characteristics, viz bond length and bond angles, were theoretically calculated and compared to experimental results. By using the DFT/B3LYP/6-311++G(d,p) basis set in IR and Raman studies, the existence of functional groups in the selected drug zolpidem has been further clarified, and the results were compared to experimental findings. The stretching vibration of the keto group was ascribed between 1649 cm^{-1} and 1637 cm^{-1}. A three-dimensional (3D) Hirshfeld surface (HS) and a two-dimensional (2D) fingerprint map were analyzed to better understand how the compound molecules interact with one another. The results show that the interaction bond H•••H (60.1%) makes up the majority of the interaction. The charge distribution, intramolecular interactions, local reactive centers, and possible nucleophilic and electrophilic reactive sites were analyzed by Mulliken population, NBO, and MESP analysis. Further, first-order hyperpolarizability calculations have been carried out to determine the NLO of the titled compound. In-depth molecular docking simulation was performed to confirm the potential biological effects of zolpidem by establishing a binding pattern with orexin receptors.

Keywords: Zolpidem, DFT, Vibrational properties, NBO, NLO, Molecular docking

INTRODUCTION

In recent decades, there has been a dramatically increased prevalence of sleep-related disorders in adults, with a twofold increase in older people due to demographic, biological, lifestyle, and cognitive changes, which are most commonly treated with benzodiazepines, Z-drugs, orexin, and melatonin receptor agonists [1-4]. The first benzodiazepine receptor agonist to be developed was zolpidem, also known as N, N-dimethyl-2-[6-methyl-2-(4-methylphenyl)imidazo[1,2-a] pyridin-3-yl]acetamide, which belongs to the imidazopyridine family with a molecular formula of $C_{19}H_{21}N_3O$ and molecular weight of 307.4 g mol^{-1} [5]. Zolpidem structure has an imidazopyridine ring with a tolyl group in the second position, an N,N-dimethyl-carbamoylmethyl group in the third position, and a methyl group in the sixth position. Zolpidem has structural similarities with zaleplon, zopiclone, and melatonin [6,7], and it is also a chemotherapy drug used to treat insomnia, a sleeping disorder that binds to GABAA receptors to induce sleep [8,9]. Also, zolpidem has neuroprodective, anticonvulsant, anxiolytic, and myorelaxant properties [10, 11]. The biological and pharmaceutical industries heavily rely on benzodiazepines and their derivatives. Using DFT (Density Function Theory), the antioxidant property of zolpidem was determined by Marco Bortoli *et al*., [12]. Jemberk *et al.,* suggest that zolpidem has a neuroprotective effect by preventing p19 neurons against glutamate toxicity by modulating the p13k/Akt pathway [13].

Hypocretin, a G protein-coupled receptor, is another name for orexin receptors, which regulate many signaling processes, including sleep-wake rhythm, energy balance,

*Corresponding author. E-mail: sselvaphy@gmail.com

stress response, glucose metabolism, and feeding behavior. When orexins bind to orexin receptors, these results in activating downstream second messengers, including protein kinase B, phospholipases, adenylyl cyclases, and mitogen-activated protein kinases, as well as raising the level of cytosolic calcium, thereby decreasing oxidative stress and increasing neuro production. As a result, orexin receptor antagonists may have important therapeutic value [14,15]. For the analysis of organic molecules, especially biologically active molecules, the computational calculations are very useful to know about the crystal clear picture of the molecule in all aspects, as found further in the previous reports [16-25]. A careful survey of the literature revealed the absence of a comprehensive theoretical and experimental spectroscopic characterization of the structure of zolpidem. The present communication deals with a detailed theoretical and experimental spectroscopic investigation of zolpidem to get structural and spectroscopic insights. In addition, the biological importance of zolpidem was confirmed by molecular docking studies.

MATERIALS AND METHODS

Sample and Experimental Details

The 98% pure powder form of zolpidem was obtained from Sigma Aldrich Co., Chemical, USA, and it was used without any additional modification for recording. Using a Perkin Elmer Two FT-IR/ATR spectrometer with 1.0 cm^{-1} resolution, the zolpidem FT-IR spectrum was captured between 4000 cm^{-1} and 400 cm^{-1}. The Raman spectrum of zolpidem was also recorded in the mid-IR region and collected using an RFS-27 FT-Raman spectrometer from Bruker with a resolution of 2 cm^{-1} and an excitation wavelength of 1064 nm from an Nd: YAG laser.

Computational details

Without any geometric restrictions, the theoretical calculations for zolpidem were calculated at the DFT/B3LYP level of theory [26-28] using the 6-311++G(d,p) basis set at Gaussian 09 W software [29]. For zolpidem, the molecular electrostatic potential surface, vibrational frequencies, Mulliken charges, thermodynamic characteristics, and molecular geometry optimizations were identified. The same theoretical level has been used to calculate natural bond orbitals (NBO), frontier molecular orbitals (FMO), and nonlinear optical (NLO). Combining the results of the Chemcraft program [30], allows for a highly accurate graphic depiction and enables the prediction of the vibrational assignments. Using the Argus lab software, the molecule electrostatic potential was visualized [31]. Using the VEDA 4 tool, the PED analyses were computed [32]. To further understand intermolecular interactions, 2D fingerprint plots of zolpidem and HS analyses were created using the Crystal Explorer 3.1 program [33].

Molecular Docking

An effective tool to determine the binding affinity among ligands with targets is molecular docking, which was performed between orexin receptors and zolpidem using AutoDock4 software [34]. Protein data bank with PDB ID: 4S0V was used to determine the orexin receptor X-ray crystal structure, and it is a major target for many hypnotic drugs and benzodiazepines. After removing the water molecules from the target, an OPLS-2005 force with an RMSD of 0.30 was employed for some minimization. The structure of the compound was derived from three-dimensional structures in XML format, and it was then minimized via impact energy minimization utilizing 5000 cycles of conjugate gradient and 1000 cycles of steepest descent.

RESULTS AND DISCUSSION

Geometrical Description

The optimized geometrical skeletal and atom labeling of zolpidem are shown in Fig. 1. The findings of the theoretical computation of bond length and angles using DFT are provided in Table S1 (Supplementary material) along with a comparison to experimental data from the literature [35]. The optimized molecular structure of zolpidem reveals eight different types of bond angles, and the compound also contains four distinct bond lengths. The bond length of 1.22 Å is typically predicted to keto group (C_{13}=O_1). The optimum bond length is theoretically calculated to be 1.222 Å and is actually observed to be 1.205 Å. G.J. Georges *et al*. reported that the C=O bond length as 1.244 Å shows good agreement with the expected value [36]. Whereas, the bond angles of O_1-C_{13}-N_4 and O_1-C_{13}-C_8 were computed at 122.3°, 120.8° and experimentally observed at

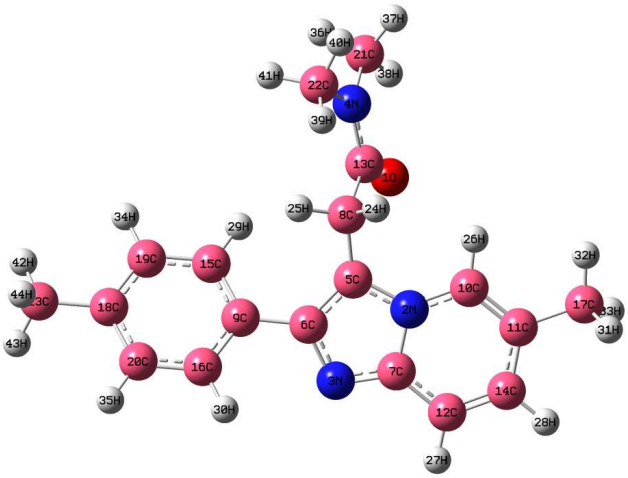

Fig. 1. Optimized molecular structure of zolpidem.

122.6°, 121.2° respectively. The lengths of the N-C bonds are theoretically between 1.326 Å and 1.459 Å, while they are actually between 1.334 Å and 1.449 Å. According to G.J. Georges *et al*., the N-C bond distance falls between 1.325 Å and 1.393 Å. The computed bond angles for Carbon-Nitrogen-Carbon and Nitrogen-Carbon-Carbon ranged from 106-131°, 105.0-130.9° and experimentally observed at 107.3-130.5°, 104.9-131.5°. The literature predicts that, the bond lengths of C-C as well as C=C have expected values around 1.45 Å and 1.35 Å [37].

The theoretically predicted C-C bond length has values in the range of 1.394-1.540 Å and experimental values in the range of 1.344-1.535 Å. These values were well in line with an earlier report of 1.382-1.500 Å that was reported by G.J. Georges *et al.* It is found that the C_8-C_{13} bond distance is higher than the expected range because of the oxygen atom impact. However, C=C has theoretical and experimental values of 1.366-1.400 Å and 1.344-1.394 Å. The experimental bond angle value of C-C-C is 134.6-108° whereas theoretically this value is found to be in the range 107.9-131.3°. Similarly, the N-C-C angle has an experimental and theoretical value of 117.3°/118°. The theoretically computed and experimental Carbon-Hydrogen bond lengths are 1.080-1.097 Å and 0.925-1.022 Å respectively. The computed bond angles of Nitrogen-Carbon-Hydrogen, Hydrogen-Carbon-Hydrogen, and Carbon-Carbon-Hydrogen are in the range of 108.8-111.6°, 107.9-123.9°, 105.9-107.9° and the experimental values are 109.1-110.3°, 108.7-121.3°, and 106.5-109.6°. The experimental data is in excellent agreement with the computed values, showing a linear coefficient value of 0.98827 for lengths and 0.9483 for angles. Moreover, there is a strong correlation between the two sets of values. The correlation chart between observed and simulated values is presented in Fig. S1 (Supplementary material). According to the data, the C_{13}-N_4-C_{22} variable (≥5°) has the highest difference (between experimental and estimated values) since optimization was carried out in isolated form.

Vibrational Analysis

The most important tasks in the field of organic chemistry are vibrational spectroscopy. Zolpidem contains 44 atoms and 126 vibration modes based on (3N-6) vibration degree of freedom. The findings of the observed Raman and IR measurements are contrasted with the theoretical values derived from computer approaches. The calculated and experimental vibration spectrum of zolpidem is exposed in Figs. 2 and 3. The vibration spectrum of zolpidem shows CH, CH_3, CH_2, CO, CC, and CN stretching and bending vibrations. Table S2 (supplementary material), provides complete theoretical and experimental wave numbers. The theoretical wavenumbers are often larger than the observed wavenumbers because of electron correlation effects and basis set restrictions. In order to obtain the scaled theoretical wavenumbers for all vibrations, a scaling factor of 0.96 has been applied [38]. Simulated Raman scattering activity (Si) acquired using the Gaussian 09 W software was converted into Raman intensity using the following formula [38,39].

$$I_R = \frac{f(v_o - v_i)^4 S_i}{v_i[1 - \exp - hcv_i/kt]}$$

CH Vibrations

It is typical to expect CH stretching vibrations in the region of 3000-3100 cm^{-1} [40] in aromatic compounds. The bands are not overdone by the make-up of the substituents since Nitrogen-Hydrogen and Carbon-Hydrogen vibrations emerge in this region at frequencies higher than Carbon-Oxygen and Carbon-Nitrogen vibrations. Expected stretching vibrations in the tiling compound include those for modes C_{10}-H_{26}, C_{12}-H_{27}, C_{15}-H_{29}, and C_{16}-H_{30},

C_{19}-H_{34}, and C_{20}-H_{35}. According to the results of the investigation, CH stretching vibrations are experimentally observed at 3234 cm^{-1} in the Raman, 3345 cm^{-1} in the infrared spectrum, and 3092, 3079, 3066, 3053, 3044, 3028, 3027 cm^{-1} in theoretical calculations, with PED values of 98%, 100%, 96%, 98%, 89%, 100%, and 98%, respectively. The region 1300-1000 cm^{-1} is predicted for the in-plane bending mode of CH [41]. This region has discrete bands that are weak to medium in strength. The FT-IR and FT-Raman spectra obtained by experiment at 1166 and 1260 cm^{-1} and 1119, 1190, and 1263 cm^{-1} are in good agreement with theoretical calculations of the CH in-plane deformation vibrations in the range of 1049-1290 cm^{-1}. Out-of-plane deformation often results in vibrations between 1000 and 750 cm^{-1} [42]. The CH out-of-plane deformations were measured and assigned, respectively, to weak bands at wavelengths of 776, 876, and 898 cm^{-1} in the Infrared spectrum and 850, 876, and 915 cm^{-1} in the Raman spectrum.

CH_2 Vibrations

There are two stretching vibrations and four bending vibrations that can happen in the methylene group [43,44]. It is possible to detect the asymmetric and symmetric stretching of CH_2 at 3100-3000 cm^{-1} and 3000-2900 cm^{-1}, respectively. In the Raman spectrum of zolpidem, the methylene symmetric stretching absorbance was detected at 2887 cm^{-1} as opposed to 2868 cm^{-1} in the theoretical spectrum with an 88% PED. In the Infrared and Raman spectra, the asymmetric stretching vibration was detected and assigned a wavelength of 2977 cm^{-1} whereas theoretical calculation computed this vibration at 2967, 6947, and 2935 cm^{-1} with PEDs of 100%, 68%, and 36%, respectively. The bending vibrations are discernible below 1500 cm^{-1} [45]. The CH_2 group has two in-plane deformation vibrations as well as two out-of-plane deformations. The rocking frequencies were found at 916, 840 cm^{-1} and observed at 898, 876 cm^{-1} in the IR spectrum and 876, 850 cm^{-1} in the Raman spectrum. In the infrared and Raman spectra, the scissoring modes were experimentally seen at 1426 cm^{-1} and 1413 cm^{-1} and simulated at 1467, 1457, 1444, and 1430 cm^{-1}. The estimated ranges for the wagging and twisting CH_2 out-plane bending modes are, 1315-1365 cm^{-1} and 1140-1180 cm^{-1} respectively [46]. Theoretical DFT assigned wagging modes to the zolpidem bands positioned at 1418, 1367, and 1290 cm^{-1}, as well as the corresponding experimental bands discovered at 1361 in FT-IR spectra. In addition, theoretical calculations of infrared twisting modes were predicted at 1206, 1191, and 1145 cm^{-1} as well as experimental measurements at 1166 cm^{-1}.

CH_3 Vibrations

The four methyl groups found in zolpidem are also known as electron-donating substituents. Nine fundamental vibrations, including symmetric and asymmetric stretching, in-plane and out-of-plane, symmetric and asymmetric deformation modes, are anticipated in the CH_3 group. The methyl stretching vibrations, both symmetric and antisymmetric, were typically recorded between 2870 and 2980 cm^{-1} [47]. Theoretically, the symmetric modes of the CH_3 were calculated in the present work at 2901, 2897, 2890, and 2881 cm^{-1}, with PEDs of 97, 100, 98, and 96%, respectively. They were empirically found in the IR and Raman spectra at 2900 cm^{-1} and 2916 cm^{-1}, respectively. The methyl group antisymmetric frequencies were empirically discovered as a medium peak at 2977 cm^{-1} in both the infrared and Raman spectra and computed at 2977, 2974, 2946, and 2940 cm^{-1} with PEDs of 99, 97, 89, and 95%. The antisymmetric and symmetric bending frequencies were found at ranges of 1390-1370 cm^{-1} and 1465-1440 cm^{-1} respectively [48]. The IR wavelength for the asymmetric deformation of the methyl group in zolpidem was determined to be 1426 cm^{-1}. Theoretical calculations place it between 1507 and 1401 cm^{-1}. In the experimental FT-Raman spectrum, the symmetric bending was detected, assigned as a strong absorbance at 1385 cm^{-1}, a very weak absorbance at 1361 cm^{-1}, a medium absorbance at 1384 cm^{-1}, and theoretically computed in the range of 1406-1384 cm^{-1}, respectively.

C-C and C=O Vibrations

Carbon-Carbon stretching vibrations, which are a highly distinctive band for aromatic compounds, have been seen in the range of 1650 and 1200 cm^{-1} [49]. According to the current analysis, these bands were observed in the experimental IR spectrum at 1538 cm^{-1} and the Raman spectrum at 1616 cm^{-1}, respectively, and were theoretically estimated to be in the range of 1646 and 1256 cm^{-1}. According to a survey of the literature, the carbon-oxygen stretching frequencies are the typical peak of the carbonyl

group, which primarily appears in the region 1600-1800 cm^{-1}. A single peak from the current investigation was found in the experimental IR spectra with medium absorbance at 1637 cm^{-1} and simulated at 1649 cm^{-1} with a PED of 86%, showing good agreement with the experimental data.

CN Vibrations

Zolpidem contains three nitrogen atoms, and it is particularly challenging to pinpoint the CN vibration since the mixing of numerous bands will manifest in a similar area. The carbon-nitrogen stretching vibrations typically range in frequency from 1382 to 1266 cm^{-1} [50]. Theoretically, the range of the current investigation CN stretching vibrations was calculated at 1384, 1367, 1338, and 1248 cm^{-1} with PEDs of 18%, 26%, and 28%, respectively. In the IR spectrum, they were observed and categorized as having a medium absorbance peak at 1341 cm^{-1} and a weak intensity peak at 1345 cm^{-1}. In Fig. S2 (supplementary material), a correlation graph between simulated and experimental wavenumbers was displayed. The difference between observed and simulated values was determined to be 0.8612 by applying the RMS method and the following equation. With (R2) of 0.9965 and 0.9965, respectively, the calculated and observed wavenumbers showed good agreement.

$$RMS = \frac{1}{n-1}\sum_{i=1}^{n}(v_i^{cal} - v_i^{exp})^2$$

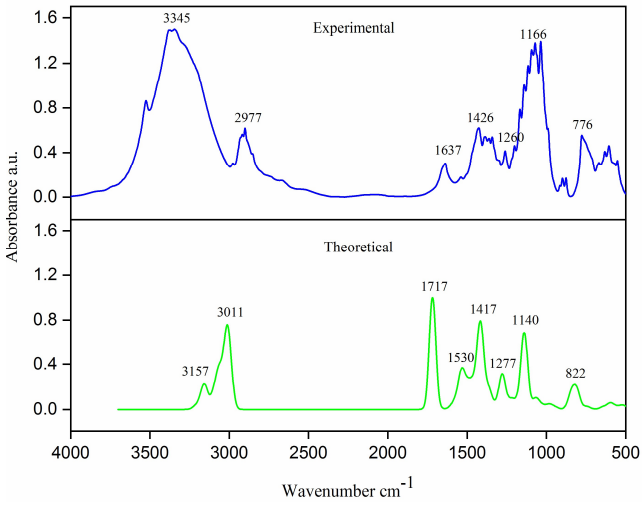

Fig. 2. Comparison between calculated and observed IR spectrum of zolpidem.

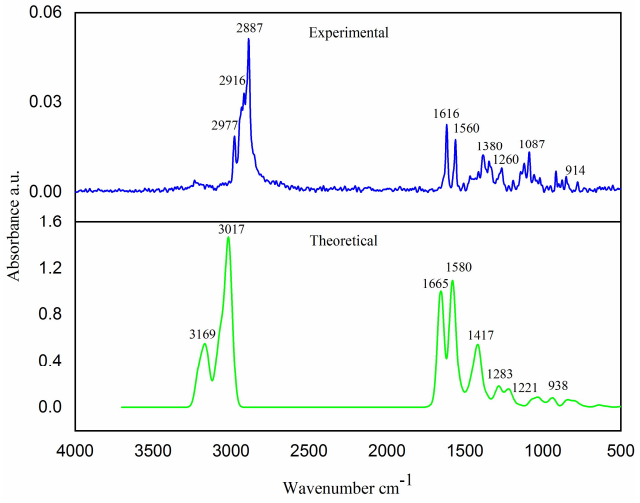

Fig. 3. Comparison between calculated and observed Raman spectrum of zolpidem.

Hirshfeld Surface Analyses

The investigation of hydrogen bonds, intermolecular interactions, and compound surfaces can be done through Hirshfeld surface (HS) analysis. HS studies and 2D fingerprint plots of zolpidem were made with the software Crystal Explorer version 3.1 [33]. The Cambridge Crystallographic Data Centre provided the CIF for the drug zolpidem (CCDC) [35]. The percentage of contributions is illustrated in Fig. 5. From the present investigation, the red and blue region in d_{norm} indicates shorter and greater amounts of *van-der-Waals* radii, the d_{norm} surfaces have been simulated in the range of 0.1278 (red colour) to 1.3489 (blue colour), and the dark, visible red surfaces denote hydrogen bonding contacts shown in Fig. 4. In zolpidem, the 2D fingerprint plots show diverse interactions of C•••C (3.3%), C•••H (11.5%), C•••N (0.3%), H•••C (8.2%), H•••H (60.1%), H•••N (4%), H•••O (3.7%), N•••C (0.3%), N•••H (4.6%), and O•••H (4%). From the results, H•••H shows the maximum contribution, and a second large contribution was obtained by the H•••C interaction. The blue and red colors in the shape index that correspond to "π-π" interactions in the structure provide the same information about curvature.

Mulliken Charges

The molecular characteristics of compounds are controlled by the distribution of atomic charges; the Mulliken

population analysis plays a crucial role in the quantum chemical computations of molecular systems. The Mulliken charges of zolpidem were computed by DFT, and the charges of individual atoms in the aforementioned molecule were visually represented in Fig. S3 (supplementary material). From the present investigation, all the hydrogen and nitrogen atoms were positively charged, especially H_{24} (0.20457e), which has a higher positivity due to the influence of the oxygen atom, which supports the electronegative nature of oxygen. In the imidazopyridine, carbons were all negatively charged except C_7 (0.352479e) with two negatively charged nitrogen atoms, and C_{11} (0.455816e) due to attached with electron-donating substituent CH_3 methyl group. In the tolyl group, all carbon atoms have negative charges except C_9 (0.692301e) and C_{18} (0.494643e), and all carbon atoms in the N,N-dimethylcarbamoylmethyl group have net negative charges. By comparing with all other atoms, C_5 (-0.061899e) exhibits less negative charge, while N_3 exhibits less positive charge, which is also supported by MESP.

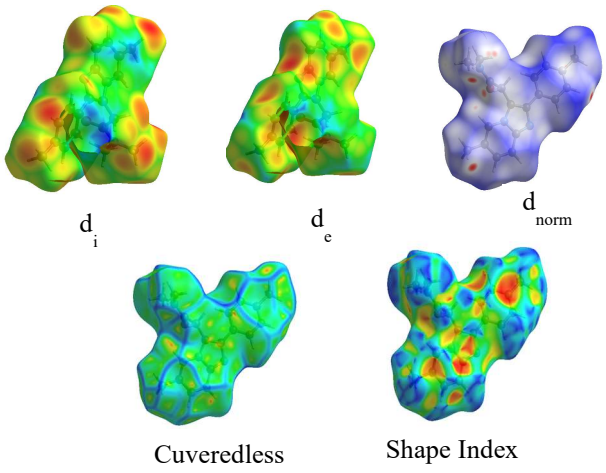

Fig. 4. HS analysis of d_i, d_e, curvedness, shape index, and dnorm of zolpidem.

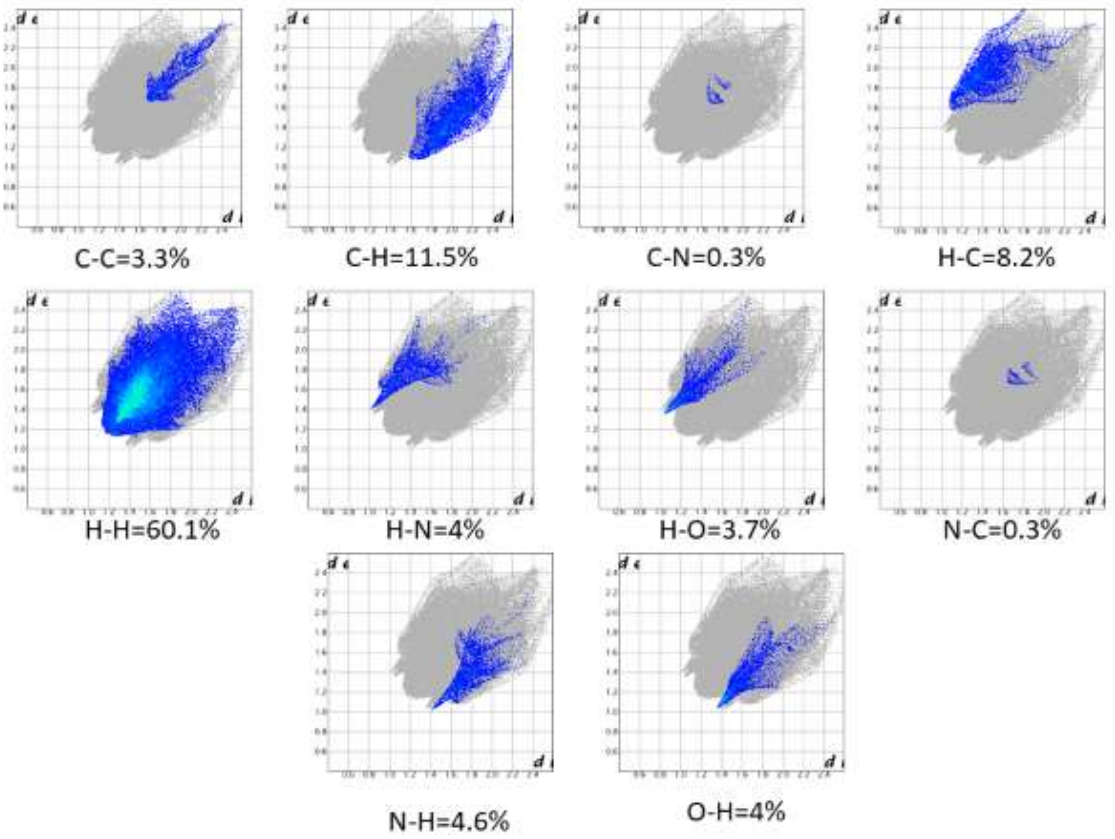

Fig. 5. The 2D fingerprint histogram of zolpidem.

MESP

Using different hues, such as red, green, yellow, orange, and blue, dependent on electron density, MESP is utilized to study hydrogen bonding, positive, negative, and neutral electrostatic potential. Blue signified the strongest attraction, high potential, and lack of electrons, whereas red indicated the highest repulsion, low potential, and abundance of electrons [51]. The ESP map of the compound is depicted in Fig. 6, where the colour codes range from 0.0500 - -0.0500 a.u. According to the current study, the area around oxygen and nitrogen atoms is colored red and is proposed to be a target for electrophilic attack and nucleophilic reactive species, while the area around hydrogen atoms is white and a target for electrophilic reactive sites, which are ideal for nucleophilic attack. The results are fairly consistent with the Mulliken population study that was previously analyzed.

NBO

The NBO approach is a method for transferring charges between molecules and figuring out how bonds in molecular systems interact. It also gives researchers in the biomedical and scientific fields a good starting point for their work. The second-order perturbation energy analysis is important in understanding molecular systems and has been effectively applied to a variety of systems to clarify the relationship between electronic structure and reactivity. The findings of the NBO analysis from the current investigations are described in Table S3 (Supplementary material). From the present findings, the π N_3-C_7→π*C_5-C_6 ($E^{(2)}$ = 25.40 kcal mol^{-1}), C_5-C_6→π*N_3-C_7($E^{(2)}$ = 12.65 kcal mol^{-1}), C_9-C_{15}→π*C_{18}-C_{19} ($E^{(2)}$ = 20.05 kcal mol^{-1}), C_{10}-C_{11}→π*C_{12}-C_{14} ($E^{(2)}$ = 15.48 kcal mol^{-1}), C_{12}-C_{14}→ π*N_3-C_7 ($E^{(2)}$ = 21.93 kcal mol^{-1}), C_{16}-C_{20}→π*C_{18}-C_{19} ($E^{(2)}$ = 21.58 kcal mol^{-1}), C_{18}-C_{19}→π*C_9-C_{15} ($E^{(2)}$ = 21.05 kcal mol^{-1}), it is clear the abovementioned interactions are responsible for molecular surface's polarity to change, which in turn affects the chemical reactivity.

Thermodynamical Properties

Thermodynamical characteristics of zolpidem show the total thermal energy is 241.172. (kcal mol^{-1}). According to calculations, the vibrational and zero-point vibrational energies are 239.938 and 227.707 kcal mol^{-1}, respectively. Total thermal energy is calculated at 241.172 kcal mol^{-1}.

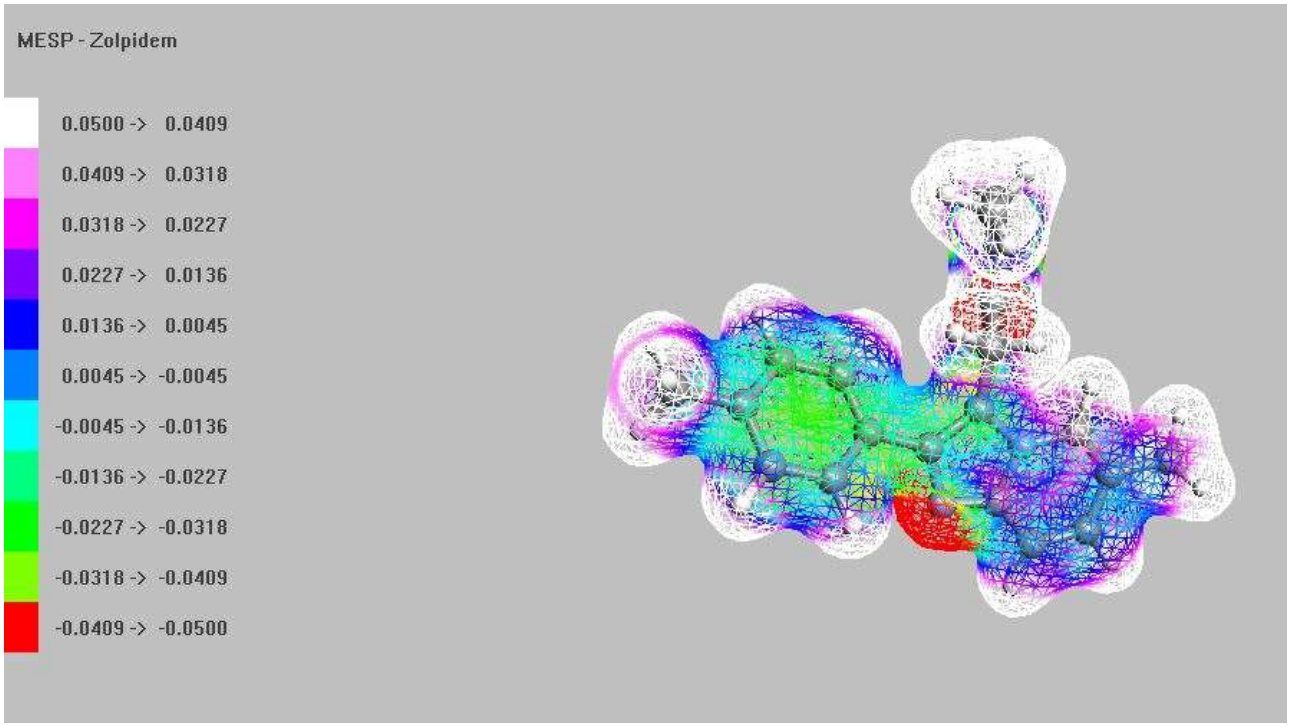

Fig. 6. MESP analysis of zolpidem.

According to calculations, the vibrational and zero-point vibrational energies are 239.938 and 227.707 kcal mol^{-1}, respectively. The amount of energy required to increase a substance's temperature by one degree is known as its heat capacity. The movement of the dipole reveals the charge distribution. Further data reveals that the specific heat capacity is 82.968 and the entropy is 163.073 cal mol^{-1} K^{-1}. The total dipole moment is predicted to be 5.5502, with the Y direction having the largest dipole moment of 4.3373. Rotational constants are calculated to be 0.32153, 0.17980, and 0.12111 for X, Y, and Z directions, respectively. Future research on zolpidem can use thermodynamic characteristics to roughly predict the orientations of chemical processes.

NLO (Non-linear optical) Properties

Quantum chemistry computations have been shown to be an effective way to figure out molecular NLO properties on a budget. Optical communication and computing work well when organic molecules are used to change photonic signals. In recent years, organic compounds, especially those with aromatic parts that speed up charge transfer through p-electron delocalization, have become very popular. From the present investigations, Table 1 displays the findings of the first-order hyperpolarizability computations. The dipole moment has a significant impact on the nonlinear activity of the molecule. It is observed from the results that the dipole moment is highly active in the Y direction with the value 4.1778 Debye, followed by the X direction with the value 3.2975 Debye. The total dipole moment is computed to be 5.3708 Debye, which is 3.911 times that of urea. The total polarizability is computed as 125.6654×10^{-24} e.s.u., which is 33.644 that of urea. The average first-order hyperpolarizability of zolpidem was 93.1901×10^{-31} e.s.u., which is 24.991 times greater than the NLO response of urea [52-53]. According to the results, zolpidem is a desirable material for upcoming non-linear optical application investigations.

Table 1. First-order Hyperpolarizability, Second Order Perturbation of Zolpidem

Parameters	DFT value	Parameters	DFT value
μ_x	0.7198	β_{xxx}	20.7536
μ_y	4.1778	β_{xxy}	-22.2129
μ_z	3.2975	β_{xyy}	13.7299
μ (D)	5.3708	β_{yyy}	89.3225
α_{xx}	-117.8080	β_{zxx}	3.6421
α_{xy}	-5.2380	β_{xyz}	16.6414
α_{yy}	-120.9986	β_{zyy}	9.9998
α_{xz}	2.5009	β_{xzz}	1.3732
α_{yz}	3.6856	β_{yzz}	17.0058
α_{zz}	-141.1897	β_{zzz}	4.3386
α_{total} (esu)	-125.6654	β_{total} (esu)	93.1901

Frontier Molecular Analysis

The HOMO and LUMO orbitals have a significant impact on the molecular chemical stability, as well as the chemical reactivity and the relative hardness and softness of the molecule. These orbitals in the compound are a pair of orbitals, which is what enables them to interact with one another in the most potent way. It has been determined that the HOMO energy is -0.20473 eV, while the LUMO energy is -0.04104 eV. The energies contribute to the explanation of hyperpolarizability *via* the utilization of intramolecular charge transfer. The energy gap, denoted by the symbol (ΔE), is an essential component of the stability index that describes the chemical reactivity of compounds. It has been determined that the HOMO-LUMO energy gap is 0.16369 eV. A lower value of energy for a compound specifies that the compound has poor kinetic stability or is more reactive. At the B3LYP/6-31++G(d) level of theory, the FMOs have been explored. Figure 7 provides information on the corresponding energy levels of the FMOs for the titled compound that was investigated; we have found that the equivalent electronic transfers occurred between the HOMO and the LUMO. Table S4 (supplementary material), lists all the electronic parameters obtained from HOMO-LUMO energy values. According to the Mayr equation theoretical interpretation, molecular nucleophilicity is correlated with the energy of its HOMO, which is based on the FMO theory and the Eyring equation of the transition state theory. On the

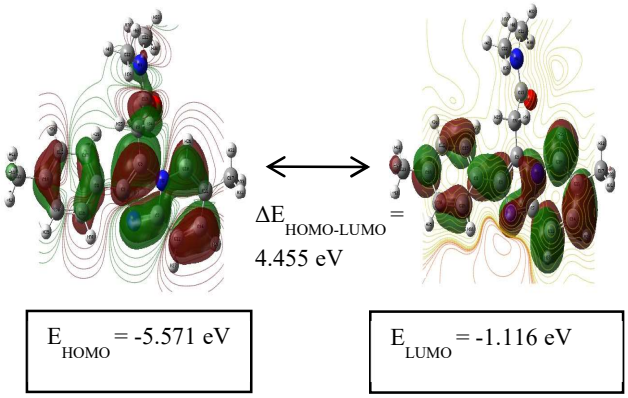

Fig. 7. HOMO-LUMO energy gap plot of zolpidem.

other hand, molecular electrophilicity is correlated with the energy of the electrophile lowest unoccupied molecular orbital, which is based on the transition state theory. The present compound has more ΔE which makes the material more stable for optical devices such as solar cells.

Molecular Docking

Orexin receptors are members of the GPCR family, which regulates many biological functions such as sleep-wake rhythm, energy balance, stress response, glucose metabolism, and feeding behavior [54]. The interaction scores between ligand and receptor were listed in Table S5 (Supplementary material), and molecular docking plots of zolpidem against the orexin receptor are visualized in Figs. 8 and 9. The detailed intermolecular interaction between orexin receptors and zolpidem was investigated. Two hydrogen bonds were formed with the carbonyl group of zolpidem and receptor amino acids arginine 328 and lysine 327, with a glide score of -33.823 and bond distances of 2.94 and 3.06 Å respectively. Meanwhile, hydrophobic interactions were also formed with the amino acids valine 325, phenylalanine 346, leusine 320, methionine 191, valine 209, proline 131, tryptophan 120, tyrosine 343, alanine 110, and cysteine 210 in the receptor and zolpidem. When compared with co-crystal suvorexant, zolpidem shows good interaction with the orexin receptor, which confirms the potential antagonist property of zolpidem with the orexin receptor and is evidence that zolpidem induces sleep by inhibiting the binding of orexin to the receptor.

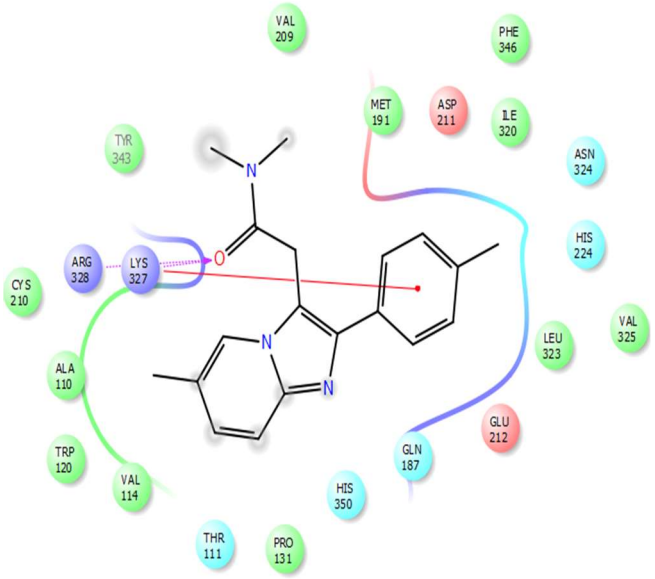

Fig. 8. Molecular docking of orexin receptor with zolpidem.

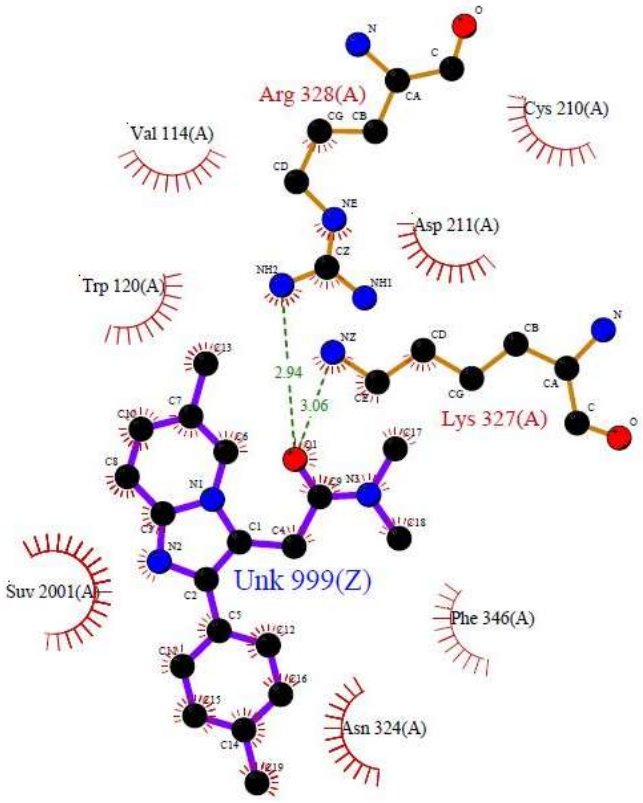

Fig. 9. Two-dimensional LigPlot view of zolpidem against orexin receptor.

CONCLUSION

Zolpidem has been subjected to spectroscopic, structural, and biological characteristics that were studied through experimentation and theoretical investigation. Analysis and comparison of optimized structural parameters with experimental values reveals a strong correlation, with linear coefficient values of (R^2 = 0.98827) for the bond length, and (R^2 = 0.9483 Å) for bond angles. The CN, CH, CO, CH_3, CC, and CH_2 stretching and bending frequencies of zolpidem are confirmed by its calculated and observed vibrational spectra. The percentage of intramolecular interaction is shown by the HS analysis with finger plots, which reveals that O•••H, C•••N, N•••H, and C•••C bonding have short contacts. It is feasible to forecast the potential reactivity tendency of zolpidem by looking at the highest stabilization of interaction energy in the molecule resonance at electron donating from LP(1) $N_4 \rightarrow \pi^*(O_1\text{-}C_{13})$ with 63.70 Kcal mol^{-1} energy. The simulated dipole moment and first-order hyperpolarizability reveal the NLO characteristics of zolpidem. The HOMO-LUMO energy gap, electron affinity, molecular hardness, and dipole moment are all very essential physical characteristics for determining the chemical reactivity and biological activities of zolpidem was examined. The results of Mulliken population and MESP analysis suggest the most advantageous site for nucleophilic attack region around hydrogens and electrophilic attack region around electronegative atoms. The biological significance of zolpidem is confirmed by the molecular docking research of the drug, which demonstrates binding affinity, hydrogen bonds, and hydrophobic contact between the ligand and target. Also, the outcomes will assist researchers in conducting in-depth biological investigations on zolpidem.

REFERENCES

[1] Machado, F. V.; Louzada, L. L.; Cross, N. E.; Camargos, E. F.; Dang-Vu, T. T.; Nobrega, O. T., More than a quarter century of the most prescribed sleeping pill: systematic review of zolpidem use by older adults. *Exp. Gerontol*. **2020**, *136* (7-8), 110962, DOI: 10.1016/j.exger.2020.110962.

[2] Low, T. L.; Choo, F. N.; Tan, S. M., The efficacy of melatonin and melatonin agonists in insomnia-An umbrella review. *J. Psychiatr. Res*. **2020***, 121*, 10-23, DOI: 10.1016/j.jpsychires.2019.10.022

[3] Patel, D.; Steinberg, J.; Patel, P., Insomnia in the elderly: a review. *J. Clin. Sleep. Med*. **2018**, *14* (6), 1017-1024, DOI: 10.5664/jcsm.7172.

[4] Sys, J.; Van Cleynenbreugel, S.; Deschodt, M.; Van der Linden, L.; Tournoy, J., Efficacy and safety of non-benzodiazepine and non-Z-drug hypnotic medication for insomnia in older people: a systematic literature review. *Eur. J. Clin. Pharmacol*. **2020**, *76* (3), 363-381, DOI: 10.1007/s00228-019-02812-z.

[5] Hasegawa, K.; Wurita, A.; Nozawa, H.; Yamagishi, I.; Minakata, K.; Watanabe, K.; Suzuki, O., Fatal zolpidem poisoning due to its intravenous self-injection: Postmortem distribution/redistribution of zolpidem and its predominant metabolite zolpidem phenyl-4-carboxylic acid in body fluids and solid tissues in an autopsy case. *Forensic. Sci. Int*. **2018**, *290*, 111-120, DOI: 10.1016/j.forsciint.2018.06.044.

[6] Hesse, L. M.; von Moltke, L. L.; Greenblatt, D. J., Clinically important drug interactions with zopiclone, zolpidem and zaleplon. *CNS drugs*, **2003**, *17* (7), 513-532, DOI: 10.2165/00023210-200317070-00004.

[7] Sadat Yousefsani, B.; Akbarizadeh, N.; Pourahmad, J., The antioxidant and neuroprotective effects of Zolpidem on acrylamide-induced neurotoxicity using Wistar rat primary neuronal cortical culture. *Toxicol. Rep*. **2020**, *7*, 233-240, DOI: 10.1016/j.toxrep.2020.01.010.

[8] Crestani, F.; Martin, J. R.; Mohler, H.; Rudolph, U., Mechanism of action of the hypnotic zolpidem *in vivo*. *Br. J. Pharmacol*. **2000**, *131* (7), 1251-1254, DOI: 10.1038/sj.bjp.0703717.

[9] Monti, J. M.; Spence, D. W.; Buttoo, K.; Pandi-Perumal, S. R., Zolpidem's use for insomnia. *Asian. J. Psychiatr*. **2017**, *25*, 79-90, DOI: 10.1016/j.ajp.2016.10.006.

[10] Sanger, D. J., The pharmacology and mechanisms of action of new generation, non-benzodiazepine hypnotic agents. *CNS drugs*, **2004**, *18* (1), 9-15, DOI: 10.2165/00023210-200418001-00004.

[11] Eslami, S. M.; Ghasemi, M.; Bahremand, T.; Momeny, M.; Gholami, M.; Sharifzadeh, M.; Dehpour, A. R., Involvement of nitrergic system in anticonvulsant effect of zolpidem in lithium-pilocarpine induced status

epilepticus: evaluation of iNOS and COX-2 genes expression. *Eur. J. Pharmacol*. **2017,** *815*, 454-461, DOI: 10.1016/j.ejphar.2017.10.002.

[12] Bortoli, M.; Dalla Tiezza, M.; Muraro, C.; Pavan, C.; Ribaudo, G.; Rodighiero, A.; Tubaro, C.; Zagotto, G.; Orian, L., Psychiatric disorders and oxidative injury: antioxidant effects of zolpidem therapy disclosed in silico. *Comput. Struct. Biotechnol. J*. **2019**, *17*, 311-318, DOI: 10.1016/j.csbj.2019.02.004.0

[13] Jembrek, M. J.; Radovanovic, V.; Vlainic, J.; Vukovic, L.; Hanzic, N., Neuroprotective effect of zolpidem against glutamate-induced toxicity is mediated *via* the PI3K/Akt pathway and inhibited by PK11195. *Toxicology*, **2018**, *406*, 58-69, DOI: 10.1016/j.tox.2018.05.014.

[14] Pallais, J. P.; Kotz, C. M.; Stanojlovic, M., Orexin/hypocretinin in multiple sclerosis and experimental autoimmune encephalomyelitis. *Neural. Regen. Res*. **2020**, *15* (6), 1039, DOI: 10.4103/1673-5374.270310.

[15] Sun, M.; Wang, W.; Li, Q.; Yuan, T.; Weng, W., Orexin A may suppress inflammatory response in fibroblast-like synoviocytes. *Biomed. Pharmacother*. **2018**, *107*, 763-768, DOI: 10.1016/j.biopha.2018.07.159.

[16] Mohd, S., Investigation on the key features of L-Histidinium 2-nitrobenzoate (LH2NB) for optoelectronic applications: A comparative study. *J King Saud Univ Sci*. **2016**, *29* (1), 70-83, DOI: 10.1016/j.jksus.2016.03.002.

[17] Mohd, A.; Mohd, S.; Baig, M. I.; Ramteke, S. P.; Muley, G. G.; AlFaify, S.; Ghramh, H. A., Experimental and computational studies of L-tartaric acid single crystal grown at optimized pH. *J. Mol. Struct.* **2018**, *1170*, 151-159, DOI: 10.1016/j.molstruc.2018.05.073.

[18] Mohammed, S.; Jain, V. K.; AlFaify, S.; Abutalib, M. M.; Yahiya, I. S.; Ajmal Khan, M., Molecular structure, spectroscopic (IR, Raman, Ultra Violet-Visible) and nonlinear optical investigation on DCBLPZ: A novel semiorganic NLO material. *J. Theor. Comput. Chem*. **2015**, *14* (8), 1550061, DOI: 10.1142/S0219633615500613.

[19] Mohd, S.; AlFaify, S.; Haider, A.; Muhammad, S., First principal studies of spectroscopic (IR and Raman, UV-visible), molecular structure, linear and nonlinear optical properties of L-arginine p-nitrobenzoate monohydrate (LANB): a new non-centrosymmetric material. *Spectrochim Acta A Mol Biomol Spectrosc*. **2015**, *147*, 84-92, DOI: 10.1016/j.saa.2015.02.111.

[20] Anbarasan, P. M.; Arunkumar, A.; Mohd, S., Computational investigations on efficient metal-free organic D-π-A dyes with different spacers for powerful DSSCs applications. *Mol Simul.* **2022**, *48* (2), 140-149, DOI: 10.1080/08927022.2021.1994965.

[21] Munusamy, A. P.; Ammasi, A.; Shajahan, S.; Ahamad, T.; Khan, M. M., Quantum chemical investigation on D-π-A-based phenothiazine organic chromophores with spacer and electron acceptor effects for DSSCs. *Struct. Chem*. **2021**, *32* (6), 2199-2207, DOI: 10.1007/s11224-021-01787-x.

[22] Arunkumar, A.; Shanavas, S.; Acevedo, R.; Anbarasan, P.M., Computational analysis on D–π–A based perylene organic efficient sensitizer in dye-sensitized solar cells. *Opt. Quantum. Electron*. **2020**, *52*, 1-13, DOI: 10.1007/s11082-020-02273-0.

[23] Arunkumar, A.; Anbarasan, P. M., Optoelectronic properties of a simple metal-free organic sensitizer with different spacer groups: quantum chemical assessments. *J. Electron. Mater*. **2019**, *48*, 1522-1530, DOI: 10.1007/s11664-018-06912-x.

[24] Arunkumar, A.; Shanavas, S.; Anbarasan, P. M., First-principles study of efficient phenothiazine-based D–π–A organic sensitizers with various spacers for DSSCs. *J. Comput. Electron.* **2018**, *17*, 1410-1420, DOI: 10.1007/s10825-018-1226-5.

[25] Balakit, A. A.; Makki, S. Q.; Sert, Y.; Ucun, F.; Alshammari, M. B.; Thordarson, P.; El-Hiti, G. A., Synthesis, spectrophotometric and DFT studies of new Triazole Schiff bases as selective naked-eye sensors for acetate anion. *Supramol Chem*. **2020**, *32* (10), 519-526, DOI: 10.1080/10610278.2020.1808217.

[26] Kohn, W.; Sham, L. J., Self-consistent equations including exchange and correlation effects. *Phys. Rev.* **1965**, *140*, A1133-A1138, DOI: 10.1103/PhysRev.140.A1133.

[27] Becke, A. D., Density functional thermo chemistry – III: The role of exact exchange. *J. Chem. Phys*. **1993**, *98*, 5648-5652, DOI: 10.1063/1.464913.

[28] Lee, C.; Yang, W.; Parr, R. G., Development of the

Colle-Salvetti correlation-energy formula into a functional of the electron density. *Phys. Rev. B*. **1988**, *37*, 785-789, DOI: 10.1103/PhysRevB.37.785.

[29] Frisch, M. J. *et al*., Gaussion 09W, Revision A.02, Gaussion Inc. Walling ford, CT, **2009**.

[30] Zhurko, G. A.; Zhurko, D. A., Chemcraft Program Version 1.6 (Build 315), **2009**, http://www.chemcraftprog.com.

[31] Thompson, M. A., ArgusLab 4.0.1 (Build 7600), **2004**, http://www.arguslab.com/.

[32] Jamroz, M. H., Vibrational energy distribution analysis VEDA 4, **2004**.

[33] McKinnon, J. J.; Turner, M. J.; Jayatilaka, D.; Spackman, M. A.; Grimwood, D. J.; Wolff, S. K., Crystal Explorer (Version 3.1). *University of Western Australia*. **2012**.

[34] Morris, G. M.; Huey, R.; Lindstrom, W.; Sanner, M. F.; Belew, R. K.; Goodsell, D. S.; Olson, A. J.; AutoDock4 and AutoDockTools4: Automated docking with selective receptor flexibility. *J. Comput. Chem*. **2009**, *30* (16), 2785-2791, DOI: 10.1002/jcc.21256.

[35] Halasz, I.; Dinnebier, R. E., Structural and thermal characterization of zolpidem hemitartrate hemihydrate (form E) and its decomposition products by laboratory x-ray powder diffraction. *J. Pharm. Sci*. **2010**, *99* (2), 871-878, DOI: 10.1002/jps.21883.

[36] Georges, G. J.; Vercauteren, D. P.; Evrard, G. H.; Durant, F. V.; George, P. G.; Wick, A. E., Characterization of the physico-chemical properties of the imidazopyridine derivative Alpidem. Comparison with Zolpidem. *Eur. J. Med. Chem*. **1993**, *28* (4), 323-335, DOI: 10.1016/0223-5234(93)90149-9.

[37] Badawi, H. M., Molecular structure and vibrational assignments of 2,4-dichlorophenoxyacetic acid herbicide. *Spectrochim. Acta A Mol. Biomol. Spectrosc*. **2010**, *77* (1), 24-27, DOI: 10.1016/j.saa.2010.04.010.

[38] Thirunavukkarasu, M.; Balaji, G.; Muthu, S.; Raajaraman, B. R.; Ramesh, P., Computational spectroscopic investigations on structural validation with IR and Raman experimental evidence, projection of ultraviolet-visible excitations, natural bond orbital interpretations, and molecular docking studies under the biological investigation on N-benzyloxycarbonyl-L-Aspartic acid 1-benzyl ester. *Chem. Data Collect.* **2021**, *31*, 100622, DOI: 10.1016/j.cdc.2020.100622.

[39] Karabacak, M.; Cinar, Z.; Kurt, M.; Sudha, S.; Sundaraganesan, N., FT-IR, FT-Raman, NMR and UV-Vis spectra, vibrational assignments and DFT calculations of 4-butyl benzoic acid. *Spectrochim. Acta A Mol. Biomol. Spectrosc*. **2012**, *85* (1), 179-189, DOI: 10.1016/j.saa.2011.09.058.

[40] Selvaraj, S.; Ram Kumar, A.; Ahilan, T.; Kesavan, M.; Gunasekaran, S.; Kumaresan, S., Multi spectroscopic and computational investigations on the electronic structure of oxyclozanide. *J. Indian Chem. Soc.* **2022**, *99* (10)*,* 100676, DOI: 10.1016/j.jics.2022.100676.

[41] Thamarai, A.; Vadamalar, R.; Raja, M.; Muthu, S.; Narayana, B.; Ramesh, P.; Muhamed, R. R.; Sevvanthi, S.; Aayisha, S., Molecular structure interpretation, spectroscopic (FT-IR, FT-Raman), electronic solvation (UV-Vis, HOMO-LUMO and NLO) properties and biological evaluation of (2E)-3-(biphenyl-4-yl)-1-(4-bromophenyl) prop-2-en-1-one: Experimental and computational modeling approach. *Spectrochim. Acta A Mol. Biomol. Spectrosc*. **2020**, *226*, 117609, DOI: 10.1016/j.saa.2019.117609.

[42] Gunasekaran, S.; Rajalakshmi, K.; Kumaresan, S., Vibrational analysis, electronic structure and nonlinear optical properties of Levofloxacin by density functional theory. *Spectrochim. Acta A Mol. Biomol. Spectrosc*. **2013**, *112*, 351-363, DOI: 10.1016/j.saa.2013.04.074.

[43] Ramalingam, M.; Jaccob, M.; Swaminathan, J.; Venuvanalingam, P.; Sundaraganesan, N., Harmonic analysis of vibrations of morpholine-4-ylmethylthiourea: A DFT, midinfrared and Raman spectral study. *Spectrochim. Acta A Mol. Biomol. Spectrosc*. **2008**, *71* (3), 996-1002, DOI: 10.1016/j.saa.2008.02.034.

[44] Thirunavukkarasu, M.; Balaji, G.; Muthu, S.; Sakthivel, S.; Prabakaran, P.; Irfan, A., Theoretical conformations studies on 2-Acetyl-gamma-butyrolactone structure and stability in aqueous phase and the solvation effects on electronic properties by quantum computational methods. *Comput. Theor. Chem*. **2022**, *1208*, 113534, DOI: 10.1016/j.comptc.2021.113534.

[45] Gulluoglu, M. T.; Erdogdu, Y.; Yurdakul, Ş., Molecular

structure and vibrational spectra of piperidine and 4-methylpiperidine by density functional theory and *ab initio* Hartree-Fock calculations. *J. Mol. Struct.* **2007**, *834,* 540-547, DOI: 10.1016/ j.molstruc.2007.01.023.

[46] Suma, N.; Aruldhas, D.; Joe, I. H.; Anuf, A. R.; Sasi, B. A., Spectroscopic, quantum chemical, QTAIM analysis, molecular dynamics simulation, docking studies and solvent effect of pyridin-2-yl oxyacetic acid herbicide and its derivatives. *J. Mol. Struct*. **2020**, *1206*, 127677, DOI: 10.1016/j.molstruc.2019.127677.

[47] Premkumar, S.; Jawahar, A.; Mathavan, T.; Dhas, M. K.; Sathe, V. G.; Benial, A. M. F., DFT calculation and vibrational spectroscopic studies of 2-(tert-butoxycarbonyl (Boc)-amino)-5-bromopyridine. *Spectrochim. Acta A. Mol. Biomol. Spectrosc*. **2014**, *129*, 74-83, DOI: 10.1016/ j.saa.2014.02.147.

[48] Ram Kumar, A.; Selvaraj, S.; Jayaprakash, K. S.; Gunasekaran, S.; Kumaresan, S.; Devanathan, J.; Selvam, K. A.; Ramadass, L.; Mani, M.; Rajkumar, P., Multi-spectroscopic (FT-IR, FT-Raman, 1H NMR and 13C NMR) investigations on syringaldehyde. *J. Mol. Struct*. **2021**, *1229*, 129490, DOI: 10.1016/ j.molstruc.2020.129490.

[49] Charanya, C.; Sampathkrishnan, S.; Balamurugan, N., Quantum mechanical analysis, spectroscopic (FT-IR, FT-Raman, UV-Vis) study, and HOMO-LUMO analysis of (1S,2R)-2-amino-1-phenylpropan-1-ol using density functional theory. *J. Mol. Liq.* **2017**, *231*, 116-125, DOI: 10.1016/j.molliq.2017.01.096.

[50] Manickavelu, T.; Govindrajan, B.; Sambantham, M.; Panneerselvam, P.; Irfan, A., Computational investigation, effects of polar and non-polar solvents on optimized structure with topological parameters (ELF, LOL, AIM, and RDG) of three glycine derivative compounds. *Struct. Chem*. **2022**, *33* (4), 1295-1319, DOI: 10.1007/s11224-022-01930-2.

[51] Selvaraj, S.; Ram Kumar, A.; Ahilan, T.; Kesavan, M.; Serdaroglu, G.; Rajkumar, P.; Mani, M.; Gunasekaran, S.; Kumaresan, S., Experimental and Theoretical Spectroscopic Studies of the Electronic Structure of 2-Ethyl-2-phenylmalonamide. *Phys. Chem. Res*, **2022**, *10* (3), 333-344, DOI: 10.22036/ PCR.2021.304087.1966.

[52] Kanagathara, N.; Senthilkumar, K.; Sabari, V.; Ragavendran, V.; Elangovan. S., "Structural and Vibrational Investigation of Benzil-(1,2-Diphenylethane-1,2-Dione): Experimental and Theoretical Studies. *J. Chem.* **2022**, *2022*, 1-11, DOI: 10.1155/2022/5968496.

[53] Senthilkumar, K.; Kanagathara, N.; Ragavendran, V.; Natarajan, V.; Marchewka, M. K., Quantum chemical computational studies of 1,3-diammonium propylarsenate: a semi organic crystalline salt. *Inorg. Nano-Met. Chem.* **2021,** *52* (10)*,* 1352-1363, DOI: 10.1080/24701556.2021.1963282.

[54] Burdakov, D., How orexin signals bias action: hypothalamic and accumbal circuits. *Brain Res*. **2020**, *1731*, 145943, DOI: 10.1016/j.brainres.2018.09.011.